Fast Data Processing of a Polarimeter-Interferometer System on J-TEXT

2016 Plasma Sci. Technol. 18 1143

(http://iopscience.iop.org/1009-0630/18/12/1143)

Fast Data Processing of a Polarimeter-Interferometer System on J-TEXT*

LIU Yukai (刘煜锴)[1,3], GAO Li (高丽)[2], LIU Haiqing (刘海庆)[1], YANG Yao (杨曜)[1], GAO Xiang (高翔)[1,3], and J-TEXT Team[2]

[1]Institute of Plasma Physics, Chinese Academy of Sciences, Hefei 230031, China
[2]Institute of Fusion and Plasma Research, School of Electrical and Electronic Engineering, Huazhong University of Science and Technology, Wuhan 430074, China
[3]University of Science and Technology of China, Hefei 230026, China

Abstract A method of fast data processing has been developed to rapidly obtain evolution of the electron density profile for a multichannel polarimeter-interferometer system (POLARIS) on J-TEXT. Compared with the Abel inversion method, evolution of the density profile analyzed by this method can quickly offer important information. This method has the advantage of fast calculation speed with the order of ten milliseconds per normal shot and it is capable of processing up to 1 MHz sampled data, which is helpful for studying density sawtooth instability and the disruption between shots. In the duration of a flat-top plasma current of usual ohmic discharges on J-TEXT, shape factor u is ranged from 4 to 5. When the disruption of discharge happens, the density profile becomes peaked and the shape factor u typically decreases to 1.

Keywords: fast data processing, polarimeter-interferometer, J-TEXT

PACS: *52.55.Fa, 52.25.Xz, 52.25.Fi*

DOI: 10.1088/1009-0630/18/12/01

(Some figures may appear in colour only in the online journal)

1 Introduction

Far-Infrared (FIR) laser diagnostics are widely applied to measure plasma electron density, current density and electron density fluctuations for tokamak plasma research [1]. A vertically-viewing, multichannel far-infrared laser-based polarimeter-interferometer system (POLARIS) was developed on J-TEXT [2−4]. As we know, the variation of the electron density profile is closely related to the confinement level of the plasma. Many physical phenomena, with the help of fast processing density data obtained from POLARIS, can be analyzed mainly in terms of density profile, such as influence of resonant magnetic perturbation on the density profile and plasma confinement, density sawtooth instability and the disruption. This paper will concentrate on electron density data processing for rapidly obtaining evolution of the density profile.

2 Principle of polarimeter-interferometer diagnostic

The three-wave technique, which was originally proposed by Dodel and Kunz [5] and first appeared on the Rijnhuizen Tokamak Project (RTP) [6], can provide a density distribution with a simultaneously measured poloidal magnetic field distribution. The Faraday rotation angle, ψ can be obtained by the following equation:

$$\psi \approx \frac{\phi_{\mathrm{R}} - \phi_{\mathrm{L}}}{2} \approx 2.62 \times 10^{-13} \lambda^2 \int n_{\mathrm{e}} B_{||} \mathrm{d}l \,. \quad (1)$$

The phase shift ϕ, which carries information of the line-integrated electron density, can be obtained by the following equation:

$$\phi \approx \frac{\phi_{\mathrm{R}} + \phi_{\mathrm{L}}}{2} \approx 2.82 \times 10^{-15} \lambda \int n_{\mathrm{e}} \mathrm{d}l. \quad (2)$$

In the above two equations, ϕ_{R} and ϕ_{L} are the phase shift of the R-wave and L-wave respectively, $B_{||}$ is the component of the poloidal magnetic field parallel to the beam trace, n_{e} is the electron density, and λ is the wavelength of the laser beam.

3 Experimental setup

J-TEXT is a circular, limiter tokamak with a major radius (R_0) of 1.05 m and a minor radius

*supported by the National Magnetic Confinement Fusion Science Program of China (Nos. 2014GB106000, 2014GB106002, and 2014GB106003) and National Natural Science Foundation of China (Nos. 11275234, 11375237 and 11505238) and Scientific Research Grant of Hefei Science Center of CAS (No. 2015SRG-HSC010)

(a) of 0.27 m [7]. The POLARIS adopts a three-wave technique with three identical laser sources. Each CHCOOH laser pumped by three CO_2 lasers operates at a wavelength of 432.5 μm, with high power output >35 mW/cavity, providing the source power for the POLARIS. The electron density resolution is 1×10^{16} m^{-3} and temporal resolution is 1 μs with phase resolution $< 0.1^{o}$ [8]. Seventeen-channels are installed on J-TEXT with a 0.03 m channel spacing.

4 Method principle

Reconstruction of the electron density profile on J-TEXT based on the inversion method has been developed by utilizing POLARIS. But in order to rapidly obtain evolution of the electron density profile, a kind of approximate method was brought into being for characterizing the electron density distribution by a single shape factor u and a scaling quantity n_{e0} which is the maximal value of the density profile, we choose the approximate profile as follows [9]

$$n_e(r) = n_{e0}\left[1-(\frac{r}{a})^u\right], \tag{3}$$

where a denotes the radius of the plasma boundary. The level of width of density also can be characterized by full width at half maximum (FWHM).

$$\mathrm{FWHM} = a\cdot 2^{1-1/u}. \tag{4}$$

We can conveniently calculate the central line-averaged density along the plasma radius

$$\overline{n_e} = \frac{1}{a}\int_0^a n_e(r)\mathrm{d}r = n_{e0}\frac{u}{u+1}, \tag{5}$$

and derive the section-averaged density $\overline{\overline{n_e}}$ in the plasma cross section

$$\overline{\overline{n_e}} = \frac{2}{a^2}\int_0^a n_e(r)r\mathrm{d}r = n_{e0}\frac{u}{u+2}. \tag{6}$$

According to Eqs. (5) and (6), the shape factor and scaling quantity n_{e0} can be analytically denoted by Eqs. (7) and (8) respectively.

$$u = \frac{2\overline{\overline{n_e}}-\overline{n_e}}{\overline{n_e}-\overline{\overline{n_e}}}, \tag{7}$$

$$n_{e0} = \frac{u+1}{u}\overline{n_e} = \frac{u+2}{u}\overline{\overline{n_e}} \quad . \tag{8}$$

However, the $\overline{n_e}$ directly derives from the phase shift ϕ of the central channel on the part of numerical calculation.

$$\overline{n_e} = \frac{\phi}{2ac_1}. \tag{9}$$

And the $\overline{\overline{n_e}}$ is defined by

$$\overline{\overline{n_e}} = \frac{\sum_{i=0}^{N}\left[\frac{1}{2}(\phi_{i+1}+\phi_i)\cdot|r_{i+1}-r_i|\right]}{\pi c_1 a^2}, \tag{10}$$

where $c_1 = 2.82\times10^{-15}\lambda$, r_i means radial position of the i-th laser beam, and N is the total number of channels.

5 Method evaluation

One of the biggest features of this fast data processing method is celerity. It is indicated that the fast data processing method calculating density profile with all time points in a shot is much faster by about three orders of magnitude than the inversion method with one time point. It usually takes on the order of ten milliseconds to obtain the evolution of the density profile of one shot. In addition, Fig. 1 depicts the comparison of density profile n_e through the inversion method (dotted line) and the approximate density profile n_e' utilizing this method (full line). According to Fig. 1, despite the existence of some error due to Shafranov shift, the results from the two methods agree well, especially for the qualitative research.

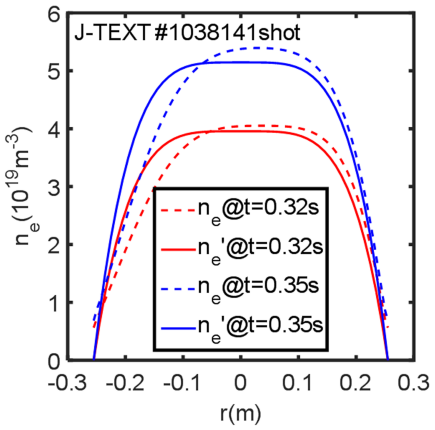

Fig.1 Comparison of electron density profile n_e and n_e' by utilizing the inversion method (dotted line) and the fast data processing method (full line), respectively

6 Method application

In recent years, the J-TEXT tokamak has been equipped with resonant magnetic perturbation (RMP) coils including static RMP and dynamic RMP in order to study the plasma response to RMP [10,11]. It has often been observed in these experiments that there is a decrease in terms of electron density caused by applied RMP, density pump-out phenomenon. In this paper, the effect of RMPs on particle confinement and the density profile is studied by means of the fast data processing method. As an example, we selected shot 1030502 with RMP for a specific explanation of this method. The pulse length of this shot is 0.77 s, plasma current is 164 kA and toroidal magnetic field is 1.8 T. In Fig. 2, the time evolutions of some plasma parameters of shot 1030502 with RMP are presented. According to Fig. 2, when penetration of the perturbation field is finished, the edge Hα radiation level and edge CIII purity level increase. The center

line-integrated density has a large decrease, however the edge line-integrated density is almost unchanged.

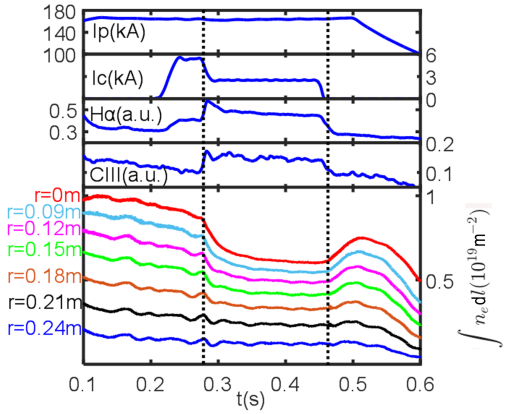

Fig.2 Time evolution of shot 1030502 with RMP. They are plasma current, current for RMP coils, edge Hα radiation, edge CIII purity level, line-integrated density at different radii

Fig. 3 portrays the space-time distribution of electron density of shot 1030502 by utilizing this fast data processing method. As shown in Fig. 3, electrons were expelled from plasma core to edge in the RMP phase of an interval of 0.27–0.46 s. Fig. 4 is the time evolution of the shape factor and FWHM of the density profile. As a key parameter for giving an index to a different density profile, the bigger the shape factor is, the broader the density profile is. It is indicated from Fig. 4 that the exhaust of electrons can be demonstrated by the increment of shape factor and FWHM, because there is no particle source. In Fig. 5, time evolutions of line-averaged, section-averaged density and maximal value of density profile are shown. In the duration of RMP, the downtrend of central line-averaged density is more serious than that of section-averaged density, which also demonstrates that there is an existence of outward electron flux due to the influence of RMP. Therefore, the evolutions of the shape factor and n_{e0} tangibly demonstrate the transportation process of particles with the characteristics of intuitive grasp and celerity.

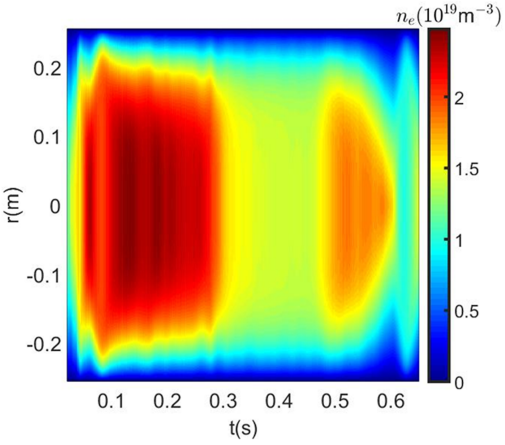

Fig.3 The space-time distribution of electron density of shot 1030502 with RMP

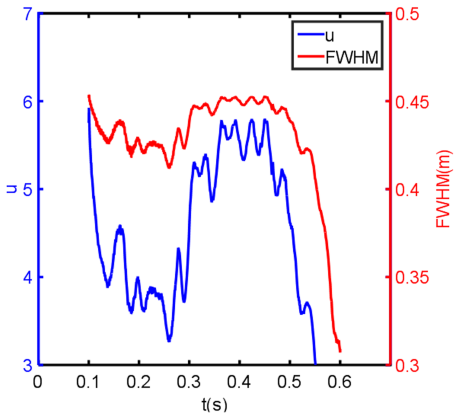

Fig.4 Time evolution of shape factor and FWHM of shot 1030502 with RMP

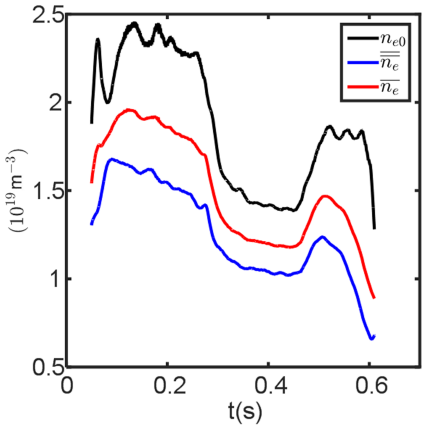

Fig.5 Time evolution of central line-averaged and section-averaged density and maximal value of density profile of shot 1030502 with RMP

In addition, it was apparent from the time evolution of shape factor and n_{e0} that the density sawtooth phenomenon emerged with a sawtooth period of 1.6 ms (see Fig. 6). It permits a good direct comprehension of particle transport effects associated with sawtooth because of the fast calculation speed of this fast data processing method. When the density crash process happens, the density profile broadens rapidly corresponding to the rapid increment of the shape factor and rapid decrease of n_{e0}. When density recovery happens, the density profile shrinks slowly. Fig. 7 shows density profiles shortly before and shortly after sawtooth crash, indicating that the density in the core rapidly drops and the density at large radii is increased slightly.

Finally, understanding of disruptions and their consequential effects is very important because disruptions can quickly expel most of the plasma thermal energy to plasma facing components with the effect of localized heating, vaporization and thermal shock damage and crack development and so on [12]. On the part of evolution of the density profile, as shown in Fig. 8, a large oscillation has been observed as a disruption precursor in the evolution of the shape factor during thermal quench, then the value of the shape factor rapidly decreases until 1 with an exhaust

of substantial particles during current quench. Large oscillation and rapid decrease are general characteristics when disruption happens on J-TEXT.

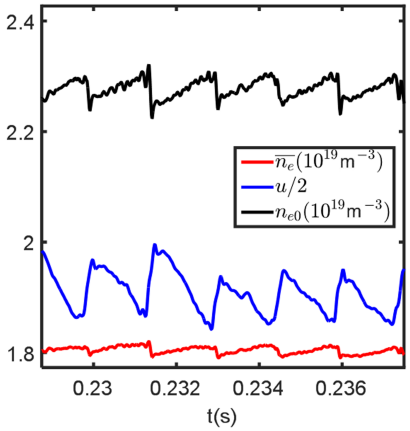

Fig.6 Time evolution of the shape factor, central line-averaged density and maximal value of density profile with small time scale of shot 1030502 with RMP

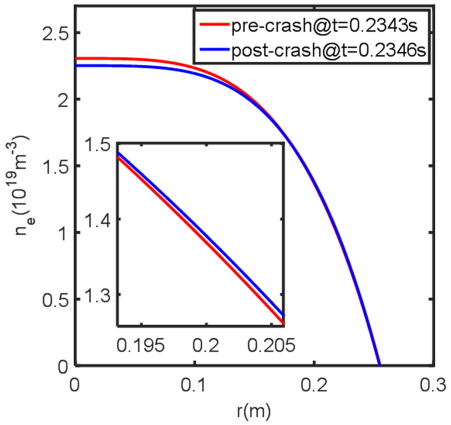

Fig.7 Density profiles shortly before and shortly after sawtooth crash

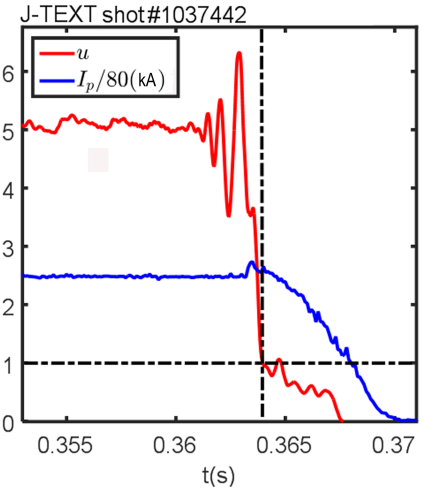

Fig.8 Typical waveforms for shape factor (red line) and plasma current (blue line) when disruption happens on J-TEXT

7 Conclusion

In this paper, the method of fast processing the density data for mainly getting the shape factor has been developed to rapidly obtain evolution of the electron density profile on J-TEXT. This method can quickly obtain the important density profile information compared with the Abel inversion method. The calculation speed of this method is very fast: the order of ten milliseconds per normal shot with up to 1 MHz sampled data. It is helpful for studying density sawtooth instability and the disruption. The influence of RMP on the density profile and plasma confinement has been analyzed with enhanced transportation mainly in view of the density profile. As a fast data processing method, it possesses the characteristics of intuitive grasp and celerity. The time evolution of the density profile is more vivid to reflect the confinement level of plasma than that of line-integrated electron density. Not only can this method provide a qualitative analysis of the density profile under various discharge conditions, but it also is used for feedback control of the density profile and is conducive to the research of sawtooth, disruption and improving plasma confinement. In ordinary ohmic discharges, shape factor u is ranged from 4 to 5. Shape factor u greatly oscillates as a disruption precursor. When the disruption of discharge happens, the density profile becomes peaked and the shape factor u typically decreases to 1.

Future plans include consideration of Shafranov shift and the problem of the asymmetric density profile; perhaps the small displacement quantity of magnetic axis (Δr) must be introduced, for a more accurate profile with characteristics of celerity and accuracy. Density profile feedback control will also be studied because there is a possibility that plasma confinement will be improved due to the control of the density profile.

Acknowledgments

The authors would like to thank the J-TEXT team for their helpful collaboration and excellent work in experiments.

References

1 Veron D. 1979, Infrared and Millimeter Waves, 2: 67
2 Zhuang G, Gentle K W, Rao B, et al. 2013, Nuclear Fusion, 53: 104014
3 Chen J, Zhuang G, Wang Z J, et al. 2012, Review of Scientific Instruments, 83: 10E306
4 Zhuang G, Chen J, Li Q, et al. 2013, Journal of Instrumentation, 8: C10019
5 Dodel G, Kunz W. 1978, Infrared Physics, 18: 773
6 Rommers J H, Donné A J H, Karelse F A, et al. 1997, Review of Scientific Instruments, 68: 1217

7 Zhuang G, Pan Y, Hu X W, et al. 2011, Nuclear Fusion, 51: 094020
8 Chen J, Zhuang G, Li Q, et al. 2014, Review of Scientific Instruments, 85: 11D303
9 Gao X, Guo Q L. 1990, International Journal of Infrared and Millimeter Waves, 11: 1399
10 Rao B, Wang G, Ding Y H, et al. 2014, Fusion Engineering and Design, 89: 378
11 Hu Q, Zhuang G, Yu Q, et al. 2014, Nuclear Fusion, 54: 064013
12 Hender T C, Wesley J C, Bialek J, et al. 2007, Nuclear Fusion, 47: S128

(Manuscript received 22 January 2016)
(Manuscript accepted 10 May 2016)
E-mail address of corresponding author GAO Li:
gaoli@hust.edu.cn